

Synthesis, characterization and a theoretical investigation of the formation of silicon, germanium and tin azapentadiene compounds from lithium azapentadienyls

J. Alfredo Gutiérrez^{a,1}, M. Angeles Paz-Sandoval^{a,*}, J. Robles^b

^a Departamento de Química, Centro de Investigación y de Estudios Avanzados del I.P.N., Apartado Postal 14-740, Mexico DF 07000, Mexico

^b Facultad de Química, Universidad de Guanajuato, Col. Noria Alta S/N, Guanajuato 36050, Guanajuato, Mexico

Received 22 September 1999; received in revised form 10 December 1999

Abstract

A series of lithium-1-azapentadienyl compounds $\text{Li}[t\text{-Bu-N}\cdots\text{CH}\cdots\text{C}(\text{R})\cdots\text{C}(\text{R}')\cdots\text{CHR}'']$ (**1**–**5**) has been synthesized by metallation of imines $t\text{-Bu-N}=\text{CH-C}(\text{R})=\text{C}(\text{R}')\text{CH}_2\text{R}''$ [$\text{R}=\text{R}'=\text{R}''=\text{H}$ (**1**); $\text{R}=\text{Me}$, $\text{R}'=\text{R}''=\text{H}$ (**2**); $\text{R}=\text{R}''=\text{H}$, $\text{R}'=\text{Me}$ (**3**); $\text{R}=\text{R}'=\text{H}$, $\text{R}''=\text{Me}$ (**4**); $\text{R}=\text{R}''=\text{Me}$, $\text{R}'=\text{H}$ (**5**)] with lithium di-*iso*-propyl amide in a mixture of hexane–THF at low temperature. Preference for the *exo* W-shaped isomer is proposed for compounds **1**–**4**, based on their chemical derivation products with electrophiles, such as EMe_3Cl ($\text{E}=\text{Si}$, Ge , Sn). Compound **5** shows both W- [**5**(W)] and U-shaped [**5**(U)] structures in a 7:1 ratio. Ab initio calculations predict that the **5**(W) compound is more favorable than the **5**(U) by 4.7 kcal mol⁻¹. We have been examining the regio- and stereoselective azapentadienyl compounds using organometallic electrophiles such as EMe_3^+ ($\text{E}=\text{Si}$, Ge , Sn). The reactions of the preferential *EE* isomers **1**–**3** with the electrophiles generally give the addition at the terminal (C5) carbon of the azapentadienyl moiety, affording the corresponding complexes $t\text{-Bu-N}=\text{CH-CH=CH-CH}_2\text{-EMe}_3$ [$\text{E}=\text{Si}$ (**6**), Ge (**7**), Sn (**8**)]; $t\text{-Bu-N}=\text{CH-C}(\text{Me})=\text{CHCH}_2\text{-EMe}_3$ [$\text{E}=\text{Si}$ (**9**), Ge (**10**), Sn (**11**)] and the corresponding *EE* and *ZE* isomers: $t\text{-Bu-N}=\text{CH-CH=C}(\text{Me})\text{-CH}_2\text{-EMe}_3$ [$\text{E}=\text{Si}$ (**12**), (**12'**); Ge (**13**), (**13'**); Sn (**14**), (**14'**)], respectively. Complex **4** reacts highly regioselectively with SiMe_3Cl affording the *EE* isomer $t\text{-Bu-N}=\text{CH-CH=CH-(Me)CH-SiMe}_3$ (**15**), but diminished regioselectivity is observed with the corresponding Ge and Sn analogues. In contrast, attack at the central (C3) carbon is observed for **5**, giving $t\text{-Bu-N}=\text{CH-(Me)C(EMe}_3)\text{-CH=CH-CH}_3$ [$\text{E}=\text{Si}$, (**18**); Ge , (**19**)]; although the regioselectivity remains for Si and Ge derivatives, a thermodynamic rearrangement occurs for the Sn complex $t\text{-Bu-N}=\text{CH-C}(\text{Me})=\text{CH}(\text{Me})\text{CH-SnMe}_3$ (**20'**), showing the addition of $-\text{SnMe}_3$ fragment at the terminal carbon. The kinetic and thermodynamic products were established through ¹H-, ¹³C- and ¹¹⁹Sn-NMR data, along with thermal isomerization studies. Based on the computed values of density-functional theory, condensed Fukui functions derived from ab initio electronic structure calculations were computed. These are shown to be useful reactivity indexes (better than conventional atomic charges) to rationalize the observed **1**–**5** chemical derivation products with electrophiles. © 2000 Elsevier Science S.A. All rights reserved.

Keywords: Azapentadienyl compounds; Lithium azapentadienyls; Organometallic azapentadienes; Silicon; Germanium; Tin

1. Introduction

As an extension of pentadienyl anion chemistry, the reactions and structures of azapentadienyl anions have attracted attention in both organic and inorganic chemistry. Pentadienyl anions [1–3] have been shown to be

useful reagents in the preparation of interesting acyclic complexes such as open metallocenes [4–11], half-open metallocenes [7,12–14] and other half-sandwich [15–23] transition-metal complexes. Also they are valuable precursors for pentadienylsilanes and stannanes, which are capable of converting ketones or aldehydes to dienyl alcohols [24,25]. The use of silylated and tin pentadienyl complexes is of increasing importance in synthetic chemistry since they are useful intermediates in organic synthesis, either as reagents for selective transformations or as intermediates for the creation of car-

* Corresponding author. Fax: +52-5-7477113.

E-mail address: mpaz@mail.cinvestav.mx (M.A. Paz-Sandoval)

¹ Present address. Facultad de Química, Universidad de Guanajuato, Guanajuato, Mexico.

bon–carbon bonds. In the latter case, the high selectivity of the tin–carbon bond cleavage involved in direct reactions, transmetallations, or transition-metal-catalyzed couplings is well established [26]. The scope of the pentadienyl derivatives has now been extended considerably. In contrast, to the best of our knowledge, only few reports involving the analogous chemistry for azapentadienyl derivatives from silicon [27–30] and related compounds [31–35] have been published, and there are no examples of related species including germanium and tin. Then, it is of great interest to investigate the related chemistry of the azapentadienyl derivatives, and to explore the potential in transmetallation reactions in order to afford new azapentadienyl-transition metal complexes. Interesting results in this regard have been published recently [22]. The most systematic studies on experimental and theoretical chemistry of azapentadienyl lithium species have been carried out by Wuerthwein and co-workers. [36–43].

In this work, we have employed density-functional theory (DFT) reactivity indexes such as the condensed Fukui functions, computed from ab initio molecular electrostatic potential (MEP) charges to study and rationalize the observed reactivity of the azapentadienyl anions. Condensed Fukui functions for the electrophilic attacks (f_j^-) on molecules **1'–5'** (see below) were calculated, and from these, the feasibility towards an electrophilic attack on specific atomic sites, j , was derived. Implications on the possible gas-phase reactivity for these molecules are analyzed in terms of Fukui functions.

2. Results and discussion

The classical method of preparing α,β -unsaturated imine compounds by the condensation of α,β -unsaturated aldehydes in the presence of a primary amine such as *tert*-butylamine gives basically the corresponding *EE*-isomers $t\text{-Bu-N=CH-C(R)=C(R')CH}_2\text{R}''$ [$\text{R} = \text{R}' = \text{R}'' = \text{H}$ (**1**); $\text{R} = \text{Me}, \text{R}' = \text{R}'' = \text{H}$ (**2**); $\text{R} = \text{R}'' = \text{H}, \text{R}' = \text{Me}$ (**3**); $\text{R} = \text{R}' = \text{H}, \text{R}'' = \text{Me}$ (**4**); $\text{R} = \text{R}'' = \text{Me}, \text{R}' = \text{H}$ (**5**)]. Compound **1** affords a mixture of *EE*/*ZE* isomers in a ratio of 9/1 [40], while compound **4** shows a 20/1 ratio. The ^1H - and ^{13}C -NMR spectroscopic data of *EE* isomers **1–5** are presented for comparative purposes in Tables 1 and 2 according with the numbering of atoms described in Scheme 1.

2.1. Preparation of the azapentadienyl anions

Lithium azapentadienyl compounds $\text{Li}[t\text{-Bu-N}\cdots\text{CH}\cdots\text{C(R)}\cdots\text{C(R')}\cdots\text{CHR}'']$ [$\text{R} = \text{R}' = \text{R}'' = \text{H}$ (**1'**); $\text{R} = \text{Me}, \text{R}' = \text{R}'' = \text{H}$ (**2'**); $\text{R} = \text{R}'' = \text{H}, \text{R}' = \text{Me}$ (**3'**); $\text{R} = \text{R}' = \text{H}, \text{R}'' = \text{Me}$ (**4'**); $\text{R} = \text{R}'' = \text{Me}, \text{R}' = \text{H}$ (**5'**)] were prepared by metallation of imines **1–5** with

lithium di-*iso*-propyl amide in a mixture of hexane–THF at low temperature, affording yellow or orange solutions as described in Section 4. Compound **1'** has been reported previously as an almost exclusively *EE* (*exo* W-shaped) isomer [40] and we found the same conformation for compounds **2', 3'** and **4'**, according to their corresponding chemical derivation products **9–16** (Scheme 1).

NMR studies of anion **3'** show only the presence of the *EE* isomer in THF- d_8 solution; this fact allows us to discern the presence of a tautomeric equilibrium between S- and W-conformers, which could be anticipated from the mixture of the *EE*/*EZ* isomers observed after addition of the corresponding electrophile EMe_3 ($\text{E} = \text{Si}, \text{Ge}, \text{Sn}$).

Compound **5'** has two methyl substituents on C3 and C5, respectively, showing that both W- [**5'(W)**] and U-shaped [**5'(U)**] structures were present in a 7/1 ratio (Scheme 2). The U conformer is not unexpected due to the presence of methyl substituents; similar results have been observed for pentadienyl lithium compounds [44,45] and an example of U-shaped lithium azapentadienyl with phenyl groups on N, C2 and C4 atoms has already been published [31]. The high 7/1 ratio agrees with our ab initio calculation (*vide infra*) in which the W structure is lower in energy than the corresponding U from 4.7 kcal mol $^{-1}$.

2.2. Azapentadienyl derivatives from Group 14

Analytical data for azapentadienyl complexes **6–20** are described in Table 3. The reactions of the preferential *EE* isomers **1'–3'** with electrophiles $\text{EMe}_3\text{-Cl}$ ($\text{E} = \text{Si}, \text{Ge}, \text{Sn}$) generally give addition at the terminal (C5) carbon of the azapentadienyl moiety affording $t\text{-Bu-N=CH-CH=CH-CH}_2\text{-EMe}_3$ complexes [$\text{E} = \text{Si}$ (**6**) [28,30], Ge (**7**), Sn (**8**)]; $t\text{-Bu-N=CH-C(Me)=CHCH}_2\text{-EMe}_3$ [$\text{E} = \text{Si}$ (**9**), Ge (**10**), Sn (**11**)] and the corresponding *EE* and *ZE* isomers: $t\text{-Bu-N=CH-CH=C(Me)-CH}_2\text{-EMe}_3$ [$\text{E} = \text{Si}$ (**12**) [27], (**12'**); Ge (**13**), (**13'**); Sn (**14**), (**14'**)], respectively. Compounds **6** and **8** show evidence of another barely detectable isomer (< 5%). However, strong overlapping with the major *EE* isomers does not allow their identification. The minor Sn isomer shows a singlet in the ^{119}Sn -NMR at 5.82 ppm, as well as signals in ^1H -NMR at 2.02 (d, 8.6 Hz), 8.29 (d, 8.6 Hz) and 0.07 ppm for the Sn-CH_2 , N=CH and SnMe_3 hydrogens, respectively, which suggest tentatively the formation of the *ZE* isomer. Complex **4'** reacts highly regioselectively with the Me_3SiCl affording the *EE* isomer $t\text{-Bu-N=CH-CH=CH-(Me)CH-SiMe}_3$ (**15**), but regioselectivity is diminished for the corresponding Ge **16** and Sn **17** analogues (*vide infra*). The reaction with tin gives a mixture of three possible regioisomers. In contrast, attack at the central (C3) carbon is observed for **5'**

Table 1
¹H-NMR data ^a of azapentadienes (**1–5**), lithium azapentadienyls (**3'**, **5'**, **5''**) and azapentadienyl derivatives of silicon, germanium and tin (*EE*) (**6–19**, **20'**) and (*EZ*) (**12'–14'**)

	<i>t</i> -Bu	C2 (H)	C3 (R)	C4 (R')	C5 (Me) or (EMe ₃)	C5 (R'')
1 (<i>EE</i>)	1.17 s	7.78 d <i>J</i> = 8.58	6.32 ddq <i>J</i> = 15.18, 8.58, 1.32	5.77 dq <i>J</i> = 15.18, 6.60	1.59 dd <i>J</i> = 6.60, 1.32	
2 (<i>EE</i>)	1.20 s	7.79 s	1.95 s, br	5.66 m	1.57 dd <i>J</i> = 6.93, 1.24	
3 (<i>EE</i>)	1.20 s	8.18 d <i>J</i> = 9.24	6.15 m	1.68 d <i>J</i> = 1.32	1.63 s	
3' (W)	1.24 s ^b	7.42 d <i>J</i> = 13.20	5.32 d <i>J</i> = 12.57	1.92 s	4.13 s	4.38 s
	1.05 s ^c	7.22 d <i>J</i> = 12.45	4.66 d <i>J</i> = 12.81	1.75 s	3.42 d <i>J</i> = 2.56	3.70 d <i>J</i> = 3.29
4 (<i>EE</i>)	1.20 s	7.82 d	6.35 ddt <i>J</i> = 15.83, 8.57, 1.32	5.93 dt <i>J</i> = 15.83, 6.60	1.96 m	0.88 t <i>J</i> = 7.26
5 (<i>EE</i>)	1.22 s	7.82 s	1.98 s, br	5.63 t <i>J</i> = 6.92	2.02 m	0.86 t <i>J</i> = 7.42
5' (W)	1.04 s	6.77 s	1.47 s	5.92 d <i>J</i> = 14.60	1.66 dd <i>J</i> = 6.43, 1.24	4.03 dq <i>J</i> = 14.60, 6.19
5'' (U)	1.02 s	6.72 s	1.58 s	6.42 d <i>J</i> = 14.85	1.74 d	4.35 dq <i>J</i> = 14.60, 6.43
6 (<i>EE</i>)	1.18 s	7.88 d <i>J</i> = 7.92	6.29 ddd <i>J</i> = 15.17, 7.92, 1.32	6.05 dt <i>J</i> = 15.17, 8.58	1.50 dd <i>J</i> = 8.58, 1.32	–0.06 s
7 (<i>EE</i>)	1.25 s	7.91 d <i>J</i> = 8.58	6.39 dd <i>J</i> = 15.18, 8.58	6.06 dt <i>J</i> = 15.18, 8.58	1.60 d <i>J</i> = 8.58	0.08 s
8 (<i>EE</i>)	1.24 s	7.90 d <i>J</i> = 8.75	6.36 dd <i>J</i> = 14.92, 9.24	6.16 dt <i>J</i> = 15.17, 9.90	1.71 d <i>J</i> = 9.90 <i>J</i> = 48.82 ^{d,e}	0.02 s <i>J</i> = 51.46 ^d , 54.10 ^e
9 (<i>EE</i>)	1.25 s	7.88 s	1.97 s	5.85 t <i>J</i> = 8.57	1.61 d <i>J</i> = 8.57	–0.02 s
10 (<i>EE</i>)	1.26 s	7.91 s	2.02 s, br	5.90 dt <i>J</i> = 9.15, 1.24	1.71 d <i>J</i> = 8.91	0.11 s
11 (<i>EE</i>)	1.25 s	7.88 s	1.99 d <i>J</i> = 1.32 <i>J</i> = 15.2 ^{d,e}	6.98 dt <i>J</i> = 9.23, 1.32	1.84 d <i>J</i> = 9.24 <i>J</i> = 54.43 ^{d,e}	0.05 s <i>J</i> = 51.46 ^d , 54.10 ^e
12 (<i>EE</i>)	1.22 s	8.26 d <i>J</i> = 8.91	6.13 dq <i>J</i> = 8.91 <i>J</i> = 1.24	1.72 d <i>J</i> = 1.48	1.44 d <i>J</i> = 0.74	–0.10 s
12' (<i>EZ</i>)	1.23 s	8.15 d <i>J</i> = 8.91	6.16 dq <i>J</i> = 1.23	1.61 d <i>J</i> = 1.48	1.70 s, br	–0.05 s
13 (<i>EE</i>)	1.24 s	8.27 d <i>J</i> = 8.79	6.15 dq <i>J</i> = 9.15, 1.10	1.72 d <i>J</i> = 1.10	1.61 d <i>J</i> = 0.73	0.06 s
13' (<i>EZ</i>)	1.25 s	8.15 d <i>J</i> = 8.79	~6.15 d <i>J</i> = 9.15	1.67 d <i>J</i> = 1.10	1.86 s, br	0.11
14 (<i>EE</i>)	1.20 s	8.21 d <i>J</i> = 8.91	6.10 dd <i>J</i> = 8.91, 0.99	1.70 d <i>J</i> = 1.24	1.70 s, br <i>J</i> = 68.28 ^{d,e}	–0.01 s <i>J</i> = 50.97 ^d , 53.20 ^e
14' (<i>EZ</i>)	1.20 s	8.09 d <i>J</i> = 8.16	5.91 dd <i>J</i> = 8.16, 1.24	1.61 d <i>J</i> = 1.24	2.02 s, br <i>J</i> = 65.15 ^d , 70.27 ^e	0.04 s <i>J</i> = 50.97 ^d , 53.20 ^e
15 ^f (<i>EE</i>)	1.27 s	7.97 d <i>J</i> = 8.58	6.44 ddd <i>J</i> = 15.17, 8.57, 1.32	6.13 dd <i>J</i> = 15.17, 7.26	1.56 quint <i>J</i> = 7.26	1.02 d <i>J</i> = 7.26
16 ^f (<i>EE</i>)	1.23 s	7.92 d <i>J</i> = 8.42	6.36 ddd <i>J</i> = 15.74, 8.42, 1.10	6.13 dd <i>J</i> = 15.74, 8.06	1.76 quint <i>J</i> = 6.96	1.04 d <i>J</i> = 6.96
18 ^f (<i>EE</i>)	1.17 s	7.64 s	1.31 s	5.95 dq <i>J</i> = 15.84, 1.32	5.25 dq <i>J</i> = 15.83, 6.60	1.69 d <i>J</i> = 6.60
19 ^f (<i>EE</i>)	1.19 s	7.68 s	1.39 s	6.02 dq <i>J</i> = 15.56, 1.65	5.26 dq <i>J</i> = 15.56, 6.41	1.63 dd <i>J</i> = 6.41, 1.65
20 ^f (<i>EE</i>)	1.22 s	7.85 s	1.96 d <i>J</i> = 1.24 <i>J</i> = 16.80 ^{d,e}	5.81 dd <i>J</i> = 11.38, 0.74 <i>J</i> = 19.30 ^{d,e}	2.38 dq <i>J</i> = 11.38, 6.92 <i>J</i> = 49.48 ^d , 51.71 ^e	1.23 d <i>J</i> = 6.92 <i>J</i> = 65.8 ^d , 69.0 ^e

^a Numbering of atoms as described in Scheme 1. In C₆D₆.

^b In C₆D₆.

^c In THF-*d*₈.

^d ²*J*(¹¹⁷Sn–¹H).

^e ²*J*(¹¹⁹Sn–¹H).

^f Corresponding signals for EMe₃ are singlets at –0.08, 0.03, 0.04, 0.17 and –0.01 (*J* = 49.48^d, *J* = 51.71^e Hz) ppm for compounds **15**, **16**, **18**, **19** and **20'**, respectively.

Table 2
¹³C-NMR data ^a of azapentadienes (1–5), lithium azapentadienyls (3', 5', 5'') and azapentadienyl derivatives of silicon, germanium and tin (EE) (6–19, 20') and (EZ) (12'–14')

	<i>t</i> -Bu	<i>t</i> -Bu	C2	C3	C4	C5	R	EMe ₃
1	29.8	56.7	155.8	134.3	137.6	18.0		
2	30.0	56.3	158.7	134.1	138.5	13.9	11.4	
3 ^b	30.0	56.9	152.4	127.7	143.1	26.3		
3'	32.2	53.2	150.5	91.8	144.7	96.1	21.0	
3' ^c	31.6	51.9	150.1	89.6	145.5	88.0	20.1	
4 ^d	29.9	56.7	156.0	132.0	144.3	19.6		
5 ^d	29.4	55.9	159.0	137.0	141.6	10.9	13.0	
5' (W) ^d	31.7	51.5	151.4	89.5	139.8	93.1	11.3	
5' (U) ^d	31.8	51.3	149.0	86.9	129.9	100.7	19.0	
6	30.0	56.6	156.0	131.8	140.4	24.2		–2.0
7	30.0	56.6	155.9	131.1	141.3	23.2		–2.5
8	30.1	56.4	156.0	128.9	143.2	17.9		–10.0
9	30.2	56.2	158.6	135.7	136.9	20.8	11.9	–1.5
10	30.2	56.2	158.6	135.1	137.9	20.2	11.8	–2.1
11	30.2	56.1	158.4	133.0	135.9	15.0	11.6	–9.5
12	30.1	56.8	152.3	125.7	145.6	31.7	19.5	–1.2
12' (EZ)	30.1	56.8	152.9	124.9	145.6	27.3	24.7	–0.9
13	29.5	56.3	152.4	125.0	146.5	30.8	18.4	–2.6
13' (EZ)	29.4	56.0	152.9	124.2	146.7	26.2	23.5	–2.2
14	30.2	56.6	152.3	123.4	147.8	26.7	19.1	–9.0
14' (EZ)	30.2	56.8	152.5	127.3	148.1	26.9	19.9	–9.4
15	29.2	56.6	156.1	129.4	146.7	26.7	13.3	–3.4
16	30.0	56.6	156.1	128.5	147.4	28.4	14.0	–4.1
18 ^d	30.1	56.5	161.2	39.7	134.5	121.0	17.2	–3.6
19 ^d	30.5	57.0	162.4	42.3	135.7	121.1	17.3	–4.1
20' ^d	30.2	56.2	158.2	131.4	146.9	23.2	12.3	–10.6

^a Numbering of atoms as described in Scheme 1. In C₆D₆.

^b R' = Me, δ = 18.4 (3).

^c In THF-*d*₈.

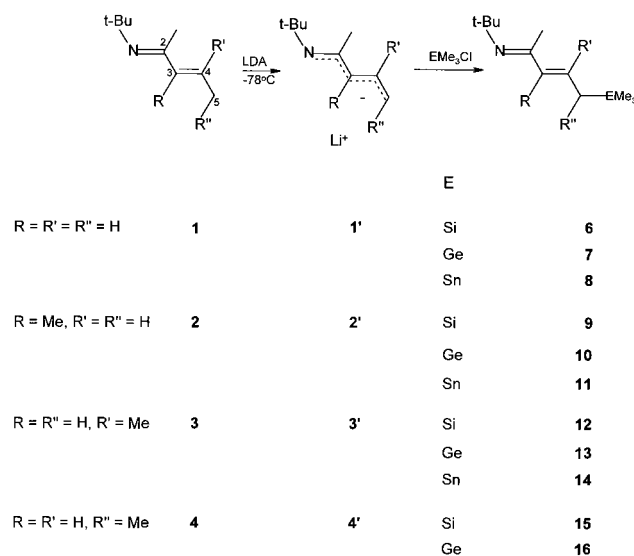
^d R'' = Me, δ = 25.8 (4); δ = 21.2 (5); δ = 18.5 [5'(W)]; δ = 18.7 [5'(U)]; δ = 18.7 (18); δ = 18.8 (19); δ = 17.5 (20').

giving *t*-Bu-N=CH-(Me)C(EMe₃)-CH=CH-CH₃ [E = Si, **18**; Ge, **19**]; although the regioselectivity remained for Si and Ge derivatives, a thermodynamic rearrangement occurs for the Sn complex *t*-Bu-N=CH-C(Me)=CH(Me)-CH-SnMe₃ (**20'**), resulting in transfer of the -SnMe₃ fragment to the terminal carbon (vide infra).

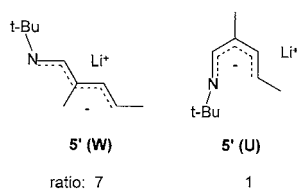
Turning attention to the alkene geometry, reactions of EMe₃Cl (E = Si, Ge, Sn) with **1'**, **2'** and **5'** proceed stereoselectively to give the *EE* isomers, while compound **3'** showed kinetic (*EE*) **12**, **13**, **14** and thermodynamic products (*EZ*) **12'**, **13'**, **14'** in a different *EE*/*EZ* ratio according to the electrophile -EMe₃ [E = Si (5.5/1); Ge (15/1); Sn (0.5/1)] (Scheme 3).

Compound **4'** shows a mixture of geometrical isomers for Ge and Sn derivatives, but while in the case of Ge there is a clear predominance of *t*-Bu-N=CH-CH=CH-(Me)CH-GeMe₃ (**16**) over other minor products, the presence of eight different tin isomers reflects a complete lack of regio- and stereoselectivity according to ¹H- and ¹¹⁹Sn-NMR (vide infra). On the other hand, the crude reaction products of all tin derivatives, except **8** and mixture **17**, shows approximately 10% of butadienamine *t*-BuNHCH=

CHCH=CH₂ (**21**) which could not be removed by distillation. Germanium derivatives **7**, **16** and **19** also show about 3% of the same by-product. Complete characterization was carried out for the unsubstituted butadien-



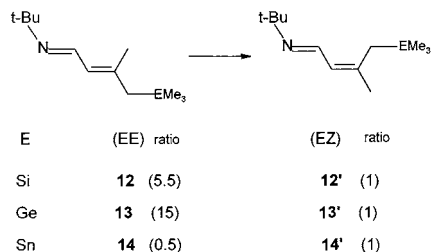
Scheme 1.



Scheme 2.

amine through ^1H -, ^{13}C -NMR, as well as from two-dimension COSY and HETCOR experiments. The amine **21** is also observed as a by-product in the transmetalation reactions between **8** and $(\text{Cp}^*\text{RuCl})_4$ [22].

It has been established that reactions of SiMe_3Cl with pentadienides give products under kinetic control because their regio- and stereoselectivities are highly geometrically and sterically dependent [44,46]. According to the reactivity of the lithium azapentadienyl complex **1'**, kinetic control is also predominant. However, the presence of a tentatively assigned *ZE* isomer for the Sn complex **8** (vide supra) suggests a geometric rearrangement giving the corresponding thermodynamic product *ZE*. Complex **2'** shows exclusive formation of *EE* products **9–11** suggesting kinetic control, while complex **3'** reacts with EClMe_3 differently, giving *EE* and *EZ* stereoisomers as already described in Scheme 3. However, the anionic lithium complex **3'** is exclusively *EE*. Then, in order to discriminate changes in the experimental procedure, a sample of **3'** was prepared and divided in three different portions, adding to each one the corresponding electrophile EMe_3Cl ($\text{E} = \text{Si}, \text{Ge}, \text{Sn}$). Under the same conditions, the crude reaction



Scheme 3.

products show through ^1H -NMR spectroscopy the same *EE/EZ* ratio as described previously (vide supra). It has been demonstrated that upon modification of the temperature of addition of the electrophiles, the ratio of *EE/EZ* isomers remains practically the same for Si (5.5/1 at -116°C and 5/1 at -78°C), while a dramatic change is observed for Sn (1/2 at -116°C and 5/1 at -78°C). These results suggest that with SiMe_3 the reaction have predominantly kinetic control, with a slight tendency to rearrange to the corresponding thermodynamic *EZ* product. With SnMe_3 the reaction shows clearly an increase of the *EE* isomer at -78°C which reflects the preference of kinetic control, while at -116°C the thermodynamic *EZ* product predominates. This observation is in agreement with previous reactions on pentadienyl derivatives [47]. In a previous study of this reaction, the exclusive formation of the kinetic *EE* product **12** was established at -15°C [27]. The lower temperature favors a low rate of consumption of the anionic azapentadienyl, which may promote the conversion of the kinetic product to the thermody-

Table 3
Analytical data of azapentadienyl derivatives of Group 14

Compound	Boiling point ($^\circ\text{C}/\text{Torr}$)	Yield (%)	Elemental analysis or HRMS ^a						Molecular formula
			Theoretical			Experimental			
			C	H	N	C	H	N	
6	51/0.04	79	66.93	11.74	7.09	66.64	11.51	7.03	$\text{C}_{11}\text{H}_{23}\text{NSi}$
7	45/0.05	68	239.1073			239.1078			$\text{C}_{11}\text{H}_{23}\text{NGe}$
8	57/0.02	66	45.87	8.04	4.86	45.62	8.13	4.66	$\text{C}_{11}\text{H}_{23}\text{NSn}$
9	38/0.05	87	68.17	11.91	6.62	67.65	10.75	6.45	$\text{C}_{12}\text{H}_{25}\text{NSi}$
10	52/0.05	78	56.31	9.84	5.47	56.23	9.92	5.38	$\text{C}_{12}\text{H}_{25}\text{NGe}$
11	55/0.05	71	299.1005			299.1004			$\text{C}_{12}\text{H}_{25}\text{NSn}$
12+12'	70/0.02	82	68.17	11.91	6.62	67.98	11.65	6.61	$\text{C}_{12}\text{H}_{25}\text{NSi}$
13+13'	60/0.02	81	56.31	9.84	5.47	56.39	9.97	5.29	$\text{C}_{12}\text{H}_{25}\text{NGe}$
14+14'	67/0.02	76	299.1008			299.1005			$\text{C}_{12}\text{H}_{25}\text{NSn}$
15	m.p. 45	78	68.17	11.91	6.62	65.37	11.27	6.26	$\text{C}_{12}\text{H}_{25}\text{NSi}$
16	m.p. 44	52	253.1229			255.1222			$\text{C}_{12}\text{H}_{25}\text{NGe}$
17^c	60/0.03	57	47.71	8.34	4.63	47.71	8.12	4.86	$\text{C}_{12}\text{H}_{25}\text{NSn}$
18	42/0.03	76	69.25	12.07	6.21	69.55	12.19	6.05	$\text{C}_{13}\text{H}_{27}\text{NSi}$
19	55/0.04	52	267.1382			267.1386			$\text{C}_{13}\text{H}_{27}\text{NGe}$
20'	72/0.04	60	313.1167			313.1161			$\text{C}_{13}\text{H}_{27}\text{NSn}$

^a High-resolution mass spectrometry. Electron impact, 70 eV.

^b Corresponding isotope used.

^c Complex mixture of eight isomers.

namic one [44]. The same effect is observed in the reaction of azapentadienyl **3'** with the organic electrophile $(\text{CH}_3)_2\text{C}=\text{C}-\text{CH}_2-\text{CH}_2-\text{Cl}$ which gives a mixture of three isomers at -78°C , but only one product at -15°C [27].

Complex **4'** reacts with EMe_3Cl ($\text{E} = \text{Si}, \text{Ge}, \text{Sn}$) giving different products depending on E; while $\text{E} = \text{Si}, \text{Ge}$ afford compounds **15** and **16**, respectively, $\text{E} = \text{Sn}$ gives a complex mixture of regio- and stereoisomers. This mixture is designated as **17** and according to ^{119}Sn -NMR involves eight different products. The reaction with GeMe_3Cl shows **16** in the crude reaction products, as the main product, along with a small amount of an analogous mixture of products, as observed for reaction with SnMe_3Cl . The Si derivative gives the cleanest reaction, showing only traces of some by-products; however, several unsuccessful attempts to separate them by distillation prevented the isolation of compound **15** completely pure. Complex **4'** showed no stereospecificity, which suggests geometrical rearrangements from the corresponding *EE* isomers to other stereoisomers. This is in contrast with the electrophilic attack towards **1'**, **2'** and **3'** in which there is evidence of kinetic control, in agreement with results obtained for analogous lithium pentadienyls [45,48,49]. This rearrangement could be favored in the presence of still unreacted lithium azapentadienyl and these results show first kinetic control, followed by a rearrangement, which finally affords the thermodynamic product. However, there is no clear evidence of a predominant species, there always being present a complex mixture of **17**. The elemental analysis corresponds to the molecular formula $\text{C}_{12}\text{H}_{25}\text{NSn}$. This mixture crystallizes as a white solid, which melts at 15°C . The reaction was carried out under different experimental conditions, involving modifying the time of addition of the electrophile, gradual increase of temperature, recrystallizations and simultaneous reactions, with similar results each time. However, by increasing the temperature at which the reactants were mixed, going from -116 to -15°C , different relative intensities of ^1H -NMR signals of the product were observed indicating different *EE/EZ* ratios of isomers in the mixtures. Finally, by reversing the order of mixing the reactants, that is, adding the anion **4'** to the electrophile

SnMe_3Cl , it is observed that a complex mixture is once again obtained. This result suggests that the azapentadienyl **4'** suffers simultaneous attack at its three nucleophilic centers by the SnMe_3Cl electrophile.

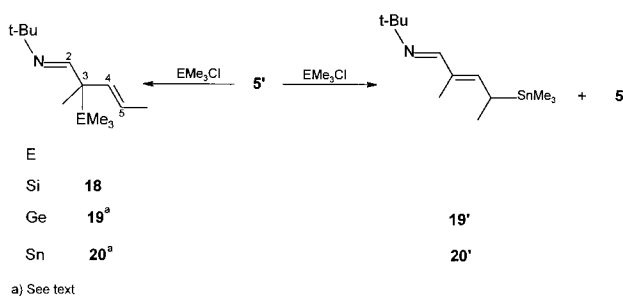
As previously mentioned, complex **5'** in the presence of EMe_3Cl ($\text{E} = \text{Si}$ and Ge) give the corresponding products **18** and **19** from attack at C3, while SnMe_3Cl gives product **20'** from attack at C5 (Scheme 4). However, if the reaction is carried out in THF–hexane in a 1/1 ratio, instead of 2/1 (see Section 4), the product appears almost exclusively as the regioisomer **20**, which can be slowly transformed to the corresponding compound **20'** during the purification process through distillation; in fact, after two distillations the transformation is complete. This suggests that **20** is the kinetic product and **20'** the thermodynamic one. As expected, in a more polar medium such as THF, unreacted azapentadienyl **5'** finds a better way to carry out the conversion of **20** to **20'**, the latter one being the only one observed. The reaction between **5'** and SnMe_3Cl is not very clean and even though **20'** is the major species present, a significant amount of the α,β -unsaturated imine **5** is observed in a 4/1 molar ratio, respectively, along with some SnMe_3Cl . Compound **20'** did not show any stereoisomers. There is also evidence of the presence of free α,β -unsaturated imine with the germanium compound **19**.

2.3. Comparative studies of the chemistry of Si, Ge and Sn

The ^1H - and ^{13}C -NMR assignments were carried out using heteronuclear correlations. Differential NOE, specifically CYCLENONE [50], was very useful in the spectral assignments for complexes **1–20**. Steric interactions between the different methyl substituents and particularly the bulky *tert*-butyl and EMe_3 groups reduced significantly the possibilities as far as stereochemistry is concerned.

Data for compounds **1–16** and **18–20** are in Tables 1 and 2. $^{119,117}\text{Sn}-^{13}\text{C}$ coupling constants from ^{13}C -NMR spectra were quite useful in the corresponding tin assignments and they are described in Table 4.

The electronegativity of the corresponding E atom in compounds **6–8**, **9–11** is reflected by the corresponding proton chemical shift for the $\text{CH}_2\text{-E}$ fragment, in which the trend observed was $\text{Sn} < \text{Ge} \sim \text{Si}$. The typical *trans* couplings ($J = 15$ Hz) between hydrogens H3 and H4 suggest the E geometry for this part of the molecule. ^{13}C -NMR spectra of complexes **9–11** show that the methyl groups on C3 are shifted to lower frequencies ($\delta = \sim 12$ ppm) as a result of the γ effect due to the presence of the $\text{CH}_2\text{-EMe}_3$ fragment in a *cis* position. The CH_2 resonance is also shifted to low frequency, and as expected, this shift is absent in compounds **6–8**. The stereochemistry was confirmed by NOE experiments (vide infra).



Scheme 4.

Table 4
Coupling constants data ^a from ¹³C- and ¹¹⁹Sn-NMR of compounds **8**, **11**, **14**, **14'** and **20'**

Compound	C2	C3	C4	C5	EMe ₃	¹¹⁹ Sn-NMR ^b
	⁴ J(^{119,117} Sn– ¹³ C)	³ J(^{119,117} Sn– ¹³ C)	² J(^{119,117} Sn– ¹³ C)	¹ J(^{119,117} Sn– ¹³ C)	¹ J(^{119,117} Sn– ¹³ C)	
8	22	46.3	50.7	256.7 ^c 268.8 ^b	314.0 ^c 326.4 ^b	δ = 2.17 ¹ J = 328.6 ¹ J' = 269.9 ² J = 47.0
11	23.1	47.2	52.8	256.7 ^c 269.9 ^b	309.5 ^c 324.0 ^b	δ = 4.19 ¹ J = 324.8 ¹ J' = 266.1 ² J = 50.8
14	17.6	44.1	50.8	262.2 ^c 274.3 ^b	309.6 ^c 325.6 ^b	δ = 5.24 ¹ J = 324.7 ¹ J' = 273.9
14'	19.8	40.9	50.6	257.8 ^c 269.9 ^b	309.6 ^c 325.6 ^b	δ = 8.66 ¹ J = 324.7 ¹ J' = 269.9
20'	22.9	45.0	47.4	299.6 ^c 312.8 ^b	293.2 ^c 306.4 ^b	δ = 14.75 ¹ J = 309.0

^a In C₆D₆, SnMe₄ (δ = 0 ppm).

^b Coupling constants in Hertz, ¹¹⁹Sn–¹³C.

^c Coupling constants in Hertz, ¹¹⁷Sn–¹³C.

The highest difference among ¹H-NMR spectra of the *EE* isomers for the Group 14 derivatives is observed for H5 in compound **5'**; in **18** and **19** the hydrogen H5 is olefinic and appears as a doublet of quartets at δ = 5.26 ppm with a *trans* coupling of 16 Hz with H4; for compound **20'** it is a doublet of quartets at δ = 2.38 ppm and 11.38 Hz, suggesting that C5 has sp³ character. In an analogous manner, ¹³C-NMR shows the most notable difference for C3 and C5 in **18** and **19**, which correspond to sp³ and sp² carbons, respectively, while for **20'** the opposite trend is observed.

Identical ¹¹⁹Sn-NMR spectra are observed for the crude reaction products of the complex mixture **17** before and after it has been distilled. There are five signals between 0 and 5 ppm and three signals between 45 and 55 ppm, along with a singlet at 112 ppm from SnMe₃Cl, which cannot be removed by distillation. The high-frequency signals are attributed to species with a N–SnMe₃ fragment [51] while those at low frequency correspond to C–SnMe₃ species. As each regioisomer could have four stereoisomers, 12 different isomers should be expected. Considering *ZZ* as the most sterically crowded isomer, we may have the regioisomers metallated on the nitrogen atom, and the three less bulky stereoisomers *EE*, *EZ*, *ZE* at higher frequencies (45–55 ppm), while the corresponding five signals at low frequencies may be attributed to *EE*, *EZ* and *ZE* stereoisomers of each regioisomer, *EE* being the most likely. As the NMR approach to the assignment of the multicomponent mixture **17** led to ambiguous conclusions, we attempted unsuccessfully to study the interconversion by thermal isomerization, because we

observed only decomposition products. Then, it is interesting to compare that while SiMe₃ reacts with **4'**, regio- and stereoselectively, the SnMe₃ fragment afforded a lack of selectivity and GeMe₃ displayed an intermediate behavior, more related to SiMe₃ than SnMe₃. The ¹H-NMR of the crude reaction product **16** showed around 30% of a complex mixture analogue to **17**. This fact suggests that Ge has intermediate behavior between those of Si and Sn.

The absolute tin–carbon coupling constant data for compounds **8**, **11**, **14**, **14'** and **20'** reflect the substituents' influence and the azapentadienyl geometry. Some interesting aspects are that the substitution of a methyl group on C3 showed a small effect on the corresponding ^{119,117}Sn–¹³C coupling in compounds **11** and **20'**, as compared with the non-substituted compound **8**. Alternatively, a methyl group substituted on C4, as that one observed for compounds **14** and **14'**, was found to reduce their coupling considerably. The corresponding ^{119,117}Sn coupling constants for C3 do not show a defined trend, giving evidence of the sensitivity of this carbon atom to substitution or change in geometry (Table 4).

The presence of a methyl group in C5 for compound **20'**, which is absent in compounds **8**, **11**, **14** and **14'**, affords a different coupling pattern. In the case of compound **20'** the SnMe₃ fragment shows smaller ¹J(¹¹⁹Sn–¹³C) and ¹J(¹¹⁷Sn–¹³C) values, while higher values are observed for the corresponding HC–Sn fragment (C5) with respect to compounds **8**, **11**, **14** and **14'**, the values for these last compounds being quite similar. A comparison of **20'** with the analogous compound **11**,

which does not have the methyl group on C5, allows one to establish the influence of the methyl groups on the electronic density of the Sn–C bonds. C2 and the methyl group on C3 are located four bonds from the tin atom and show $^4J(^{119,117}\text{Sn}-^{13}\text{C})$ of 22.9 and 12.1 Hz, respectively, giving evidence of the higher electronic interaction between the iminic carbon C2 and the tin atom due to the conjugation of the α,β -unsaturated system in the substituted compound **20'**. A similar pattern is observed for the olefinic carbon C4 with respect to the methyl group substituted on C5.

$^1\text{H-NMR}$ shows an increase in the absolute value for the corresponding $^2J(^{119,117}\text{Sn}-^1\text{H})$ coupling of the $\text{H}_2\text{C-Sn}$ or HC-Sn fragments going from the non-substituted compound **8** to the most substituted species **20'**. It is interesting to observe that while the coupling constant $^nJ(^{119,117}\text{Sn}-^{13}\text{C})$ increases with the conjugation, $^nJ(^{119,117}\text{Sn}-^1\text{H})$ shows an opposite effect.

Compounds **11** and **20'** show that their corresponding methyl vinylic protons, five bonds away from the tin atom, have a coupling constant around 16 Hz, while the iminic protons do not show appreciable coupling with tin. The same effect is observed for hydrogens on β carbons (relative to the Sn atom), which are three bonds away from tin in compound **20'**; the methyl group has strong couplings, $^3J(^{117}\text{Sn}-^1\text{H}) = 65.8$ Hz and $^3J(^{119}\text{Sn}-^1\text{H}) = 69.0$ Hz, while the vinylic proton shows a considerably smaller and not very well resolved $^3J(^{119,117}\text{Sn}-^1\text{H})$ coupling constant of 19.3 Hz. This behavior could be due to hyperconjugation and the hybridization of the corresponding carbon atoms. In fact, coupling constant values in $^{119}\text{Sn-NMR}$ may be rationalized according to some Karplus-like correlations [51].

2.4. Thermal isomerization studies

There is evidence of a complex mixture of regio- and stereoisomers only for **17**, while most of other compounds **6–11**, **15**, **16**, **18–20** are found as one predominant isomer, as a result of kinetic control. According to these results, we were interested in the study of the thermal isomerization, in order to know if the azapentadienyl could transform in other regio- and/or stereoisomers.

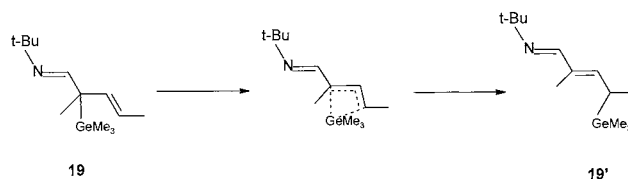
The azapentadienyl complexes **6–19** and **20'** in C_6D_6 were sealed in NMR tubes under vacuum. All samples were heated at 60°C for 4–6 h, and checked by $^1\text{H-NMR}$. After that, samples were heated at the same temperature for 3–7 days, and then the temperature was increased on 20°C until the transformation of the azapentadienyl complexes commenced. The highest temperature used was 160°C . However, only compounds **6**, **8**, and **19** showed interesting changes. The rest of the compounds did not show isomerization, even

at higher temperatures, at which they decomposed.

Compound **8**, which was present predominantly as an *EE* isomer, showed after heating at 72°C an increase of the thermodynamic *ZE* product, along with the corresponding free *ZE* imine. These experimental results reflect the isomerization and decomposition reactions of **8**, respectively. The signals at 2.03 and 8.28 ppm were increasing as a result of the *ZE* isomer **8**, while a doublet of doublets at 1.64 and a doublet at 8.31 ppm were assigned to the free *ZE* imine by comparison with the *EE* imine [40]. Similar decomposition products were observed for compounds **11**, **14**, **14'** and **20'**, but in all these cases there was no isomerization of the corresponding *EE* imine **2**, **3**, **5**.

Compound **6** shows similar behavior to **8**, after heating for 48 h at $70\text{--}80^\circ\text{C}$. There is a small, but evident, growth of signals at 8.46 and 1.78 ppm, which are from the minor *ZE* isomer, along with signals at 8.30 and 1.67 ppm from the *ZE* isomer of the free imine, and additionally, a set of five new signals in the region between 4.6 and 5.9 ppm is observed that corresponds to the butadienamine **21**, which formally represents the isomerization of both double bonds in the free imine **1**. Apparently, the higher temperature that is required in order to isomerize compound **6** afforded the isomerization of the *ZE* isomer of the free imine **1** into compound **21**.

The azapentadienyl compound **19** can be seen to isomerize to the thermodynamic regioisomer **19'**. This experiment confirms that **19** is the kinetic isomer, similar to the analogous tin compound **20** (vide supra). It is likely that transformation of **19** to **19'** and **20** to **20'** occurs through a 1,3 sigmatropic rearrangement according to Scheme 5. This kind of rearrangement has been previously observed for tin pentadienyl compounds [47]. The isomerization of **19** is very slow, showing after 4 days at 90°C new signals from the regioisomer **19'**: a doublet at 5.70 ppm ($J = 11.6$ Hz), a doublet of quartets at 2.52 ppm ($J = 7.17, 11.6$ Hz), singlets at 8.39 and 2.13 ppm. There is also evidence of a small amount of free imine **5**. After heating the mixture **19**, **19'** and **5** at 150°C during 6 weeks, we observed the formation of **19/19'** in a 1/1 ratio, along with some products of decomposition. On the other hand, compound **20** is thermally transformed by distillation (72°C) to the thermodynamic product **20'**, while the analogous Si compound **18** does not show transformation, decomposing at 160°C . As expected, these re-



Scheme 5.

sults are in agreement with the polarity of the C–E bond in the series of kinetic products **18**, **19** and **20**. Compound **20**, with the more polar bond (C–Sn), can rearrange very fast and cleanly at low temperature, while **19** (C–Ge bond) can only barely make this transformation, and **18** (C–Si bond) does not change at all, until the decomposition temperature is reached.

2.5. Mass spectrometry

Analytical evidence of compounds **7**, **11**, **16**, **20'** and a mixture of **14** and **14'** was obtained through the identification of the molecular ions by HRMS, while compounds **6**, **8**, **9**, **10**, **15**, **17**, **18**, **19** and mixtures of isomers **12**, **12'** and **13**, **13'** were studied by low resolution mass spectrometry (Table 3).

In general, the most intense fragments observed are: $[M-Me]^+$, $[M-NCMe_3]^+$, $[M-CMe_3]^+$, $[EMe_3]^+$, $[CMe_3]^+$, $[NCMe]^+$ and $[EMe]^+$. There are three basic breaking fragments: (a) E–C bond (E = Si, Ge, Sn) giving two different organometallic fragments $[M-Me]^+$ and $[EMe_3]^+$; the former is not always present, while the last one is frequently the base peak. Other common fragments are those such as $[M-EMe_3]^+$, $[M-EMe_3+H]^+$; (b) N–C(sp²) bond giving $[M-NCMe_3]^+$ and in all compounds $[NCMe]^+$ is present; (c) N–C(sp³) bond giving $[CMe_3]^+$ in all cases and $[M-CMe_3]^+$ in around half of them. It is also common to observe $[M-CMe_3+H]^+$, sometimes instead of the $[M-CMe_3]^+$ fragment.

For complexes **8**, **11**, **20'** and the mixture of isomers **14** and **14'** there is evidence of the dimer $Me_3Sn-SnMe_3$ (*m/e* 330), which gave place to Me_4Sn_2 (*m/e* 300) and Me_2Sn_2 (*m/e* 270). For silicon and germanium the analogous species were not observed.

3. Theoretical calculations and methodology

The observed reactivity of the *EE* isomers **1'**–**5'** with electrophiles was rationalized through a theoretical study described in this section.

3.1. Theoretical methodology

Reactivity indexes derived from the density-functional theory (DFT) of the electronic structure of molecules [52,53] have been very successfully applied to describe and rationalize chemical reactivity in a very broad range of applications. Frontier orbitals (HOMO and LUMO) of a chemical species are very important to define its reactivity, as Fukui et al. [54] first recognized. Large HOMO–LUMO gaps are known to provide great stability and low reactivity to a chemical species. This observation is a basic ingredient of the hard and soft acids and bases principle of Pearson [55]

which was first quantified by means of the DFT [56–58], thus establishing a sound definition of the concepts of global (as pertaining to the whole chemical species) or absolute hardness (η) and softness (S) [59–63], which are inverse to each other. Hardness is proportional to the HOMO–LUMO gap and a large η should imply stability for the chemical species.

Atomic and molecular global hardnesses have been computed by different means [64–67] and the concept of hardness has been used to understand aromaticity in organic [68,69] and organometallic molecules [70]. The relative hardness concept was introduced to characterize aromatic and *anti*-aromatic species [71] and the activation hardness index is useful to predict the orientation of electrophilic aromatic substitution in organic chemistry [72]. A very important result is the recognition that there seems to be a rule of nature requiring that molecules arrange themselves so as to be as hard as possible [73]. This has been rationalized through the principle of maximum hardness, which indicates that the equilibrium state of a chemical system is attained when η is a maximum (minimum S) [61,74–76].

One can define [77–79] regional or atomic reactivity indexes as well, such as the condensed or atomic Fukui functions for the appropriate *j*th atomic region. For instance, for an electrophilic attack on the azapentadienyl anions, the respective Fukui function is

$$f_j^- = q_j(N) - q_j(N-1) \quad (1)$$

In this equation, q_j are the atomic charges (Mulliken populations, electrostatic derived charges, or others) at the *j*th atomic site in the anionic (N), or neutral (N–1) chemical species. These local reactivity indexes have been successfully applied to rationalize reactivity in a number of chemical situations [80–88].

The purpose of this theoretical study is to apply the DFT indexes to understand the observed reactivity of the *EE* isomers **1'**–**5'** when subject to an electrophilic attack. As far as we are aware, this is the first time this approach has been applied.

3.2. Theoretical results

3.2.1. Geometry optimization

For each chemical species, we initially obtained a semi-empirical [89] PM3 geometry that in turn was used as the initial geometry to obtain a Hartree–Fock with minimum basis set (HF/STO-3G) optimized geometry. The geometry obtained was tested to correspond to an absolute potential minimum through analysis of the resulting Hessian frequencies. Keeping this geometry, we thereafter obtained single point energies and charges at a higher level of theory [89], improving the numerical basis set, namely to HF/6-31G(d).

Since it is well accepted now that charges obtained from molecular electrostatic potentials (MEPs) are bet-

Table 5
Condensed Fukui functions, f_j^- , for electrophilic attack at the j th atom, from MEP charges computed at the HF/6-31G(d)//HF/STO-3G level, for some atoms in the 1'-5' azapentadienide anions ^a

Atom	Compound 1'	Compound 2'	Compound 3'	Compound 4'	Compound 5'(U)	Compound 5'(W)
N1	-0.30	-0.31	-0.28	-0.28	-0.40	-0.31
C2	0.13	0.05	0.09	0.10	0.15	0.08
C3	-0.47	-0.31	-0.46	-0.44	-0.43	-0.34
C4	0.24	0.17	0.22	0.19	0.20	0.12
C5	-0.42	-0.39	-0.39	-0.35	-0.31	-0.29

^a Atom labeling is described in Scheme 1.

ter than the Mulliken populations [90], we consistently employed MEP charges to estimate the condensed reactivity indexes. The charges computed in this way for the anion (N) and neutral (N-1) species were used to compute the electrophilic f_j^- reactivity indexes.

All calculations were performed and visualized with the SPARTAN 5.1 program package [91]. The total energies, electrostatic charges and other molecular properties of the neutral and anionic compounds were calculated with the same (anion) geometry to ensure the condition that the external potential $v(r)$ due to the nuclei remains constant [52].

3.2.2. Reactivity parameters for 1'-5' compounds

We employed Eq. (1) to obtain the condensed Fukui functions for electrophilic attacks. In all cases the MEP-derived charges were used, at the HF/6-31G(*)/HF/STO-3G level of theory/precision. It is important to recall that steric effects are implicitly included in these reactivity indexes since they are obtained from the SCF density corresponding to the optimized geometry of the chemical species.

In Table 5, results are shown for the most important C atoms in these compounds (Scheme 1). The condensed Fukui function for electrophilic attacks are displayed for the relevant atoms in the 1'-5' compounds.

It can be observed that the largest (absolute) value of f_j^- , belongs to C5 (in compound 2') and C3 (in compounds 1', 3', 4', 5'(U) and 5'(W)). This implies that these should be the most reactive sites towards an electrophilic attack. When the theoretical results from the DFT reactivity indexes are compared with the observed reactivity of the 1'-5' azapentadienide compounds, we find complete agreement in compounds 2', 5'(U) and 5'(W). For compound 4' the theoretical prediction points to C3 as the active site towards electrophilic attack. It is hard to compare with the experiments here, since the observed reactivity is very dependent on the nature of E, leading sometimes to a complex mixture of regio- and stereoisomers. This reveals no specificity in the observed reactivity of complex 4' and a number of the observed products agree with the theoretical result. Finally, in the remaining compounds 1' and 3', the theoretically predicted active sites towards

electrophilic attack are both at C3, although the observed reactivity is at C5. Nevertheless, C5 is the second active site predicted by the calculations in both cases. For these cases the theoretical predictions would agree with initial reactions occurring under kinetic control, followed by further rearrangements in the reaction media to form the observed thermodynamic products (reactivity on C5). The DFT Fukui function reactivity indexes are *initial* reactivity predictors. Therefore, in some cases where important rearrangements may occur as in 1' and 3', the finally observed products may differ from the prediction for the initial reactivity.

In general, we can consider that the complex observed initial reactivity of the 1'-5' azapentadienide compounds is well described and in agreement with the DFT reactivity indexes, which are better than conventional atomic charges estimations for rationalizing and predicting electrophilic reactivity.

4. Experimental

Reactions were carried out under dry nitrogen atmospheres, using standard Schlenk-line techniques. Solvents were purified and dried under standard methods and were distilled under nitrogen immediately prior to use. Deuterated benzene was dried under Na and distilled. All commercial reagents from Aldrich, Baker, Merck and Strem were used without further purification.

The ¹H-, ¹³C- and ¹¹⁹Sn-NMR spectra were obtained with Jeol 90, GSX-270, Eclipse-400 and Varian Unity-300 spectrometers in CDCl₃, C₆D₆ and THF-*d*₈ solutions. All chemical shifts are reported in ppm with reference to TMS. IR spectra were recorded as films if the sample was liquid at room temperature (r.t.), but with potassium bromide pellets in the case of solids on a Perkin-Elmer 6FPC-FT spectrophotometer. Mass spectra were recorded on a Hewlett-Packard HP-5990A spectrometer operating at 70 eV and HRMS were performed at the University of Washington, St. Louis, MI, USA. Analytical data were obtained from Robertson Microlit Laboratories, Inc. in Madison, NJ, USA.

All calculations were carried out on a Silicon Graphics Octane Workstation (Dual MIPS RISC R10000 64-bit 195 MHz/1MB cache Processor, IRIX 6.4 operating system, 256 MB RAM, 4 GB Disk). The level of theory and numerical accuracy attained for our full geometry optimizations without any symmetry restrictions is at the Hartree–Fock HF/6-31G(d)//HF/STO-3G level, including all optimized geometries, wavefunctions and energies. For our calculations and visualizations, we employed the SPARTAN version 5.1 software package [91].

4.1. General method of preparation of the imines **1–5**

Preparations of imines **1–5** were carried out in essentially the same way as described elsewhere. In a 500 ml flask with a Dean–Stark trap, 0.5 mol of unsaturated aldehyde and 0.5 mol of *tert*-butylamine were refluxed in benzene (200 ml) with two drops of glacial acetic acid, until 9 ml of water were distilled in the trap. Then, 180 ml of benzene was removed and the reaction mixture washed with three portions of distilled water (20 ml). The organic fraction was dried over anhydrous magnesium sulfate, filtered and distilled under reduced pressure, obtaining the corresponding imines in yields around 70–80%.

4.2. General method of preparation of the lithium azapentadienide compounds **1'–5'**

Freshly distilled imine (32 mmol) was added dropwise to a cold (-116°C , EtOH–liq. N_2) freshly prepared lithium di-*iso*-propyl amide (LDA) [Butyllithium (32 mmol) in THF (40 ml) was added dropwise to a cold (-116°C) solution of di-*iso*-propylamine freshly distilled over solid KOH. The mixture was subsequently allowed to warm to 25°C] (32 mmol) in hexane–THF (1:2) (60 ml). The stirred mixture was subsequently allowed to warm to r.t. overnight. The corresponding lithium azapentadienyl solutions gave yellow solutions for **1'**, **2'** and **5'**, while a lemon-yellow color was observed for **3'** and an orange one for compound **4'**.

4.3. General method of preparation of the azapentadienyl derivatives of Group 14: compounds **6–19**, **20'** and **12'–14'**

A general procedure for synthesis of complexes **6–19** and **20'** was carried out as described:

To a stirred hexane–THF solution with the corresponding lithium–azapentadienyl complexes **1'–5'** (32 mmol) was added at -116°C the electrophile ECiMe_3 ($\text{E} = \text{Si}, \text{Ge}, \text{Sn}$) (33.6 mmol) in THF (5 ml). The solution changed from orange or yellow to colorless at the equivalence point. The solution was concentrated to 20 ml by evaporation, and pentane (40 ml) was added

to induce precipitation of the salt, which then was removed by filtration. The pentane solution was distilled in vacuo (0.05–0.01 mmHg, $38–71^{\circ}\text{C}$, see Table 3) to give the corresponding azapentadienyl derivatives of group 14: **6–19** and **20'** in 52–87% yields. For specific yields, elemental analysis or HRMS see Table 3.

5. Supplementary material

Mass spectral data for compounds **6–19** and **20'** are available from the authors.

Acknowledgements

We gratefully acknowledge financial support from Conacyt through projects number 25059-E, 5365-E9408, 26352-E and 166-0/PAD. J.A.G. thanks Conacyt and Universidad de Guanajuato for a grant and J.R. is grateful to DGSCA-UNAM for providing a supercomputer account. HRMS was provided by the Washington University Mass Spectrometry resource, an NIH Research Resource (Grant no. P42RR0954).

References

- [1] H. Yasuda, A. Nakamura, *J. Organomet. Chem.* 285 (1985) 15 and references therein.
- [2] P. Powell, *Adv. Organomet. Chem.* 26 (1986) 125 and references therein.
- [3] D.R. Wilson, R.D. Ernst, *Organomet. Syn.* 3 (1986) 136.
- [4] R.D. Ernst, *Chem. Rev.* 88 (1988) 1255.
- [5] R.D. Ernst, J.W. Freeman, P.N. Swepston, D.R. Wilson, *J. Organomet. Chem.* 402 (1991) 17.
- [6] T.D. Newbound, A.L. Rheingold, R.D. Ernst, *Organometallics* 11 (1992) 1693.
- [7] M.S. Kralik, L. Stahl, A.M. Arif, Ch. E. Strouse, R.D. Ernst, *Organometallics* 11 (1992) 3617.
- [8] T.E. Waldman, L. Stahl, D.R. Wilson, A.M. Arif, J.P. Hutchinson, R.D. Ernst, *Organometallics* 12 (1993) 1543.
- [9] W. Weng, A.M. Arif, R.D. Ernst, *Organometallics* 12 (1993) 1537.
- [10] W. Trakarnpruk, A.M. Arif, R.D. Ernst, *J. Organomet. Chem.* 485 (1995) 25.
- [11] T.E. Waldman, B. Waltermire, A.L. Rheingold, R.D. Ernst, *Organometallics* 12 (1993) 4161.
- [12] W. Trakarnpruk, A.M. Arif, R.D. Ernst, *Organometallics* 11 (1992) 1686.
- [13] R.W. Gedridge, J.P. Hutchinson, A.L. Rheingold, R.D. Ernst, *Organometallics* 12 (1993) 1553.
- [14] I. Hyla-Kryspin, T.E. Waldman, E. Meléndez, W. Trakarnpruk, A.M. Arif, M.L. Ziegler, R.D. Ernst, R. Gleiter, *Organometallics* 14 (1995) 5030.
- [15] J.R. Bleeke, M.K. Hays, R.J. Wittenbrink, *Organometallics* 7 (1988) 1417 and references therein.
- [16] J.R. Bleeke, S.T. Luaders, *Organometallics* 14 (1995) 1667.
- [17] J.R. Bleeke, R.J. Wittenbrink, *J. Organomet. Chem.* 405 (1991) 121.

- [18] H. Schumann, A. Dietrich, *J. Organomet. Chem.* 401 (1991) C33.
- [19] T.D. Newbound, A.M. Arif, D.R. Wilson, A.L. Rheingold, R.D. Ernst, *J. Organomet. Chem.* 435 (1992) 73.
- [20] K. Kunze, A.M. Arif, R.D. Ernst, *Bull. Chem. Soc. Fr.* 130 (1993) 708.
- [21] A.M. Arif, R.D. Ernst, E. Meléndez, A.L. Rheingold, T.E. Waldman, *Organometallics* 14 (1995) 1761.
- [22] J.A. Gutiérrez, M.E. Navarro Clemente, M.A. Paz-Sandoval, A.M. Arif, R.D. Ernst, *Organometallics* 18 (1999) 1068.
- [23] J.R. Bleeke, S.T. Luaders, D.E. Robinson, *Organometallics* 13 (1994) 1592.
- [24] D. Seyferth, J. Pornet, *J. Org. Chem.* 45 (1980) 1721.
- [25] A. Hosomi, M. Saito, H. Sakurai, *Tetrahedron Lett.* (1980) 3783.
- [26] M. Pereyre, J.-P. Quintard, A. Rahm, *Tin in Organic Synthesis*, Butterworths, London, 1987.
- [27] K. Takabe, H. Fujiwara, T. Katagiri, J. Tanaka, *Tetrahedron Lett.* (1975) 1237.
- [28] M. Bellassoued, M. Salemkour, *Tetrahedron Lett.* 34 (1993) 5281.
- [29] M. Bellassoued, M. Salemkour, *Tetrahedron* 52 (1996) 4607.
- [30] M. Bellassoued, M. Majidi, *J. Organomet. Chem.* 444 (1993) C7.
- [31] H. Ahlbrecht, D. Liesching, *Synthesis* (1976) 746.
- [32] H. Ahlbrecht, E.-O. Dueber, *Synthesis* (1980) 630.
- [33] H. Ahlbrecht, E.-O. Dueber, *Synthesis* (1982) 273.
- [34] J. Barluenga, J. Joglar, S. Fustero, V. Gotor, *J. Chem. Soc. Chem. Commun.* (1986) 361.
- [35] D.R. Armstrong, W. Clegg, L. Dunbar, S.T. Liddle, M. MacGregor, R.E. Mulvey, D. Reed, S.A. Quinn, *J. Chem. Soc. Dalton Trans.* (1998) 3431.
- [36] M. Koenemann, G. Erker, R. Froehlich, E.-U. Wuerthwein, *J. Am. Chem. Soc.* 119 (1997) 11155 and references therein.
- [37] E.-U. Wuerthwein, E. Wilhelm, B. Seitz, *Tetrahedron Lett.* 24 (1983) 581.
- [38] G. Wolf, E.-U. Wuerthwein, *Tetrahedron Lett.* 29 (1988) 3647.
- [39] F. Bauman, E.-U. Wuerthwein, *Tetrahedron Lett.* 32 (1991) 4683.
- [40] G. Wolf, E.-U. Wuerthwein, *Chem. Ber.* 124 (1991) 889.
- [41] S. Wegmann, E.-U. Wuerthwein, *Tetrahedron Lett.* 34 (1993) 307.
- [42] N. Schulte, R. Frohlich, J. Hecht, E.-U. Wuerthwein, *Justus Liebigs Annal. Chem.* (1996) 371.
- [43] H. Stakemeier, E.-U. Wuerthwein, *Liebigs Ann.* (1996) 1833.
- [44] H. Yasuda, A. Nakamura, *Polym. Prepr.* 27 (1986) 136.
- [45] H. Yasuda, M. Yamauchi, Y. Ohnuma, A. Nakamura, *Bull. Chem. Soc. Jpn.* 54 (1981) 1481.
- [46] Y. Naruta, Y. Nishigaichi, K. Murayama, *J. Org. Chem.* 56 (1991) 2011.
- [47] M.J. Hails, B.E. Mann, C.M. Spencer, *J. Chem. Soc. Dalton Trans.* (1983) 729.
- [48] M. Jones, W. Kitching, *J. Organomet. Chem.* 247 (1983) C5.
- [49] M. Jones, W. Kitching, *Aust. J. Chem.* 37 (1984) 1863.
- [50] *Varian Guide to NMR Experiments*, publishing no. 87-190140-00 Rev. B0695, 1995, p. 21.
- [51] B. Wrackmeyer, *Ann. Rep. NMR Spectrosc.* 16 (1985) 73.
- [52] R.G. Parr, W. Yang, *Density Functional Theory of Atoms and Molecules*, Oxford University, New York, 1989.
- [53] B.G. Baekelandt, A. Cedillo, R.G. Parr, *J. Chem. Phys.* 103 (1995) 8548.
- [54] K. Fukui, T. Yonezawa, H. Shingu, *J. Chem. Phys.* 20 (1952) 722.
- [55] R.G. Pearson, *Hard and Soft Acid and Bases*, Dowden, Hutchinson & Ross, Stroudsburgs, PA, 1973.
- [56] R.G. Parr, R.G. Pearson, *J. Am. Chem. Soc.* 105 (1983) 7512.
- [57] R.F. Nalewajski, *J. Am. Chem. Soc.* 106 (1984) 944.
- [58] P.K. Chattaraj, H. Lee, R.G. Parr, *J. Am. Chem. Soc.* 113 (1991) 1855.
- [59] M. Berkowitz, R.G. Parr, *J. Chem. Phys.* 88 (1988) 2554.
- [60] J.L. Gázquez, A. Vela, M. Galván, *Struct. Bond.* 66 (1987) 80.
- [61] J.L. Gázquez, *Struct. Bond.* 80 (1993) 28.
- [62] P.K. Chattaraj, A. Cedillo, R.G. Parr, *J. Chem. Phys.* 103 (1995) 10621.
- [63] R. Balawender, L. Komorowski, *J. Chem. Phys.* 109 (1998) 5203.
- [64] J. Robles, L.J. Bartolotti, *J. Am. Chem. Soc.* 106 (1984) 3723.
- [65] L. Baumer, G. Sala, G. Sello, *J. Comp. Chem.* 11 (1990) 694.
- [66] S. Liu, F. De Proft, R.G. Parr, *J. Phys. Chem. A* 101 (1997) 6991.
- [67] M.K. Harbola, R.G. Parr, C. Lee, *J. Chem. Phys.* 94 (1991) 6055.
- [68] Z. Zhou, R.G. Parr, J.F. Garst, *Tetrahedron Lett.* 29 (1988) 4843.
- [69] Z. Zhou, H.V. Navanqui, *J. Phys. Org. Chem.* 3 (1990) 784.
- [70] J.A. Chamizo, J. Morgado, P. Sosa, *Organometallics* 12 (1993) 5005.
- [71] Z. Zhou, R.G. Parr, *J. Am. Chem. Soc.* 111 (1989) 7371.
- [72] Z. Zhou, R.G. Parr, *J. Am. Chem. Soc.* 112 (1990) 5720.
- [73] R.G. Pearson, *J. Chem. Edu.* 64 (1987) 561.
- [74] R.G. Parr, P.K. Chattaraj, *J. Am. Chem. Soc.* 113 (1991) 1854.
- [75] R.G. Pearson, *J. Phys. Chem.* 98 (1994) 1989.
- [76] J.L. Gázquez, A. Martínez, F. Méndez, *J. Phys. Chem.* 97 (1993) 4059.
- [77] R.G. Parr, W. Yang, *J. Am. Chem. Soc.* 106 (1984) 4049.
- [78] W. Yang, W.J. Mortier, *J. Am. Chem. Soc.* 108 (1986) 5708.
- [79] F. Gilardoni, J. Weber, T.R. Ward, *J. Phys. Chem. A* 102 (1998) 3607.
- [80] C. Lee, W. Yang, R.G. Parr, *J. Mol. Struct. (Theochem.)* 163 (1988) 305.
- [81] R.G. Parr, W. Yang, *Annu. Rev. Phys. Chem.* 46 (1995) 701.
- [82] F. De Proft, S. Amira, K. Choho, P. Geerlings, *J. Phys. Chem.* 98 (1994) 5227.
- [83] W. Langenaeker, N. Coussement, F. De Proft, P. Geerlings, *J. Phys. Chem.* 98 (1994) 3010.
- [84] M. Galván, A. Dal Pino, J.D. Joannopoulos, *Phys. Rev. Lett.* 70 (1992) 21.
- [85] M. Galván, A. Dal Pino, J. Wang, J.D. Joannopoulos, *J. Phys. Chem.* 97 (1993) 783.
- [86] A. Dal Pino, M. Galván, T.A. Arias, J.D. Joannopoulos, *J. Chem. Phys.* 98 (1993) 1606.
- [87] F. Méndez, J.L. Gázquez, *J. Am. Chem. Soc.* 116 (1994) 9298.
- [88] S. Damound, G. Van de Woude, F. Méndez, P. Geerlings, *J. Phys. Chem.* 101 (1997) 886.
- [89] W.J. Hehre, L. Radom, P.V.R. Schleyer, J.A. Pople, *Ab Initio Molecular Orbital Theory*, Wiley, New York, 1986.
- [90] B.H. Besler, K.M. Merz, P.A. Kollman, *J. Comp. Chem.* 11 (1990) 431.
- [91] SPARTAN Version 5.1, Wavefunction, Inc. 18401 Von Karman Av. Suite 370, Irvine, CA, 1998.